JOURNAL OF OPTOELECTRONICS AND ADVANCED MATERIALS Vol. 20, No. 7-8, July – August 2018, p. 431 - 434

Growth and spectral properties of Ce^{3+}:YAG single crystal

J. HASANI BARBARAN[*], M. SASANI GHAMSARI, I. JAVAHERI, B. BAHARVAND
Photonics and Quantum Technologies Research School, Nuclear Science and Technology Research Institute, P. O. Box: 11155-3486, Tehran, Iran

---

In this study, a limited-flow of argon gas was employed to grow Ce^{3+}:YAG single crystal by Czochralski (CZ) technique. Without any reduction gas, the reduction of Ce^{4+} to Ce^{3+} can be managed and the formation of Ce^{3+} ions is achievable by this method. The X-ray diffraction (XRD) analysis, absorption and photoluminescence spectroscopy were used to study the structural and optical properties of the grown crystal. The synthesized crystal has strong emission at 527 nm. No color-center absorption and emission bands were observed in as-grown Ce:YAG crystal and it is free of usual luminescence crystalline defects.

(Received July 5, 2017; accepted August 9, 2018)

Keywords: Ce^{3+}:YAG single crystal, Czochralski method, X-ray diffraction, Scintillator materials

---

1. Introduction

Over three decades, yttrium aluminium garnet (YAG) single crystals with different dopant ions have attracted the great interests due to their application as laser or photonic materials. Different dopant ions such as Nd^{3+}, Er^{3+} and Yb^{3+} have been used to develop YAG single crystals based laser materials with enhanced optical properties. On the other hand, there are several rare earth ions such as Ce^{3+} which is used to prepare YAG based scintillation materials. This kind of optical materials are also employed as phosphors used in solid state lighting technology [1]. Among them, Ce-doped yttrium aluminium garnet is being used as a phosphor or a scintillator in many applications [2-4]. Due to the short fluorescence decay time, persistence of the scintillation and light emission in the visible spectrum resulted from very efficient 5d–4f transition of Ce^{3+} in garnet host material, the Ce-doped yttrium aluminum garnet single crystal is widely used as a scintillator and high-speed X-ray detectors [5,6]. Moreover, the excited Ce:YAG crystal can emit light at 550 nm wavelength which is well match with the sensitivity spectrum of Si photodiodes and CCD detectors [7]. Large-sized Ce:YAG scintillation crystal shows different characteristics such as good phosphorescence features, high mechanical strength, chemical stability and reasonable production cost [8]. Nevertheless, the scintillation parameters of the Ce-doped yttrium aluminum garnet single crystal are very sensitive to the growth conditions [9]. As it has been reported by Dong et al [10], the color centers and impurity defects have a significant influence on the scintillation properties of Ce:YAG crystals. It means that an optimized crystal growing process is needed to control the density of crystal defects. Usually, the traditional RF-heated Czochralski (CZ) method using an iridium crucible is employed to grow Ce:YAG scintillation. To achieve high quality large sized Ce:YAG crystals using the CZ method, the formation of the main microscopic growth defects such as bubbles, lateral core, central core and irregular inclusions must be prevented [11]. Firstly, the formation of the central and lateral core defects must be controlled. These defects are easily formed during CZ growth. Large central and lateral cores caused by the convex interface growing condition lead to the optical inhomogeneity of the crystal. The slight variations in the crystal rotation rate and fluid motion during the growth of crystal by CZ method can lead to the instability of the solid–melt interface (S/M), which can easily generate growth defects in crystals [11]. Among all of the factors that influence the interface shape, the composition of the growth atmosphere plays a vital role [12]. For example, Kim et al. [13] showed that the formation of color centers in PWO single crystals can be controlled by the crystal growth atmosphere. On the other hand, a suitable atmosphere needs to be used in growing process of Ce:YAG single crystal. That is due to the fact that the cerium oxide used as one of the starting materials is in the form of CeO_2 (Ce^{4+}). However, the cerium ions in Ce:YAG single crystal must be in the form of Ce^{3+} ions. It means that the concentration of Ce^{3+} ions in grown crystal must be taken with appropriate activity level for scintillation. Therefore, the form of cerium ions has to change to Ce^{3+} in the grown crystal. To introduce of cerium in Ce^{3+} state, the reduction growing condition was usually used when the crystal to be grown by CZ method in the controlled atmosphere. Recently, Arhipov et al [14] showed that the CO reduction atmosphere has a critical role in formation of lattice defect and quality loss of grown crystals. Depending on the growth condition of YAG family single crystals, CO interacts with YAG melt and provides carbides and oxycarbides components depositing on the thermal insulation. In addition, the use of reduction gas such as H_2 or protective atmosphere in the furnace was also reported [8, 15]. The using of H_2 consists of explosion risk. In this study, we found another way to overcome this problem. We used a limited-flow of argon gas to exhaust the excess of oxygen from the growth atmosphere instead of using the hydrogen.

2. Experimental

Cerium doped yttrium aluminium garnet single crystal (Ce^{3+}:YAG) was grown using Czochralski technique. Melting was carried out in an induction furnace with Iridium crucible. A typical pure YAG rod which is oriented in the [111] crystallographic direction was used as a seed. The growth was performed in an argon atmosphere when a limited flow of gas was emerged. High purity 99.99% Al_2O_3, Y_2O_3 and CeO_2 oxide powders were used as starting materials. The dimension of the Iridium crucible was 10 mm in diameter and length. It was located inside of the zirconia insulating cylinder in the center of the induction coil. The rotation and pulling rates were 24 rpm and 0.5 mm/hr respectively. The oxide powders were separately heated at 1300°C for 12 hr to remove the absorbed water and volatile compound. After calcination, oxide powders were stoichiometrically mixed together, pressed and sintered at 1300°C for 24 hr in air atmosphere. The atomic percent of dopant Ce in YAG sintered powder was 1%. The sintered mixed powders of component metal oxides were loaded in Iridium crucible in the crystal growth furnace. Then after melting the material and setting the temperature, a limited flow of argon gas was used for bringing out the excess oxygen. Next the seed was inserted to the melt and stabilized the temperature and started to growth of the crystal.

3. Results and discussion

Stoichiometric reaction equation was dictated that the following chemical reaction needs to take place for producing Ce^{3+}:YAG compound.

$$3(1\text{-}x)Y_2O_3 + 5Al_2O_3 + 6xCeO_2 \longrightarrow Y_{3(1\text{-}x)}Ce_{3x}Al_5O_{12} + 3/2xO_2$$

It can be found that the removing of excess oxygen is necessary for advancing the reaction and formation of the $Y_{3(1-x)}Ce_{3x}Al_5O_{12}$. This procedure helps to change Ce^{4+} ions to form of Ce^{3+} ions and the growth of Ce^{3+}:YAG. Therefore a limited flow of argon gas was employed before the inserting of a seed into the melt. The growth process was started while the temperature field was stabilized. The photo of the grown crystal is as shown in Fig. 1a. The photo of the sample with the dimensions ≈ Ø45×18 mm can be observed in Fig. 1b. It was cut from the boule of crystal. The cutting plane is perpendicular to the growth axis ⟨111⟩. The presence of scattering particles, absorption spectrum and core situation in the grown crystal were studied. By use the He-Ne laser beam was not seen any noticeable scattering particles in the sample.

Fig. 1. (a) The grown Ce^{3+}:YAG single crystal with 45 mm in diameter (b) The photo of the crystal sample after mirror polishing

Fig. 2, shows the distributions of the cores in our sample. As it can be seen in this figure, a small central core can be observed in the grown crystal. There are no any lateral and edge cores in this crystal. The position and size of the cores are very important parameters for the qualification of YAG single crystals [16].

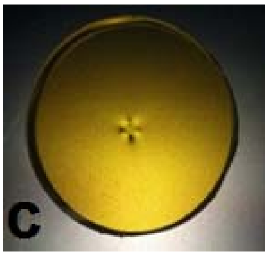

Fig. 2. Distribution of the cores in grown crystal sample

Fig. 3 displays the X-ray diffraction pattern of the prepared powders from the grown crystal. The pattern is in good agreement with the YAG phase 01-072-1315 reference code. In as-prepared sample the location of XRD peaks are almost the same as that of pure YAG. Therefore the structure of obtained crystal is bcc same as the pure YAG [17]. However, the intensity of X-ray diffraction peak is different in two patterns. By analytical method and based on the XRD results the lattice constant was calculated for the grown crystal which is equal to 12.0301 Å.

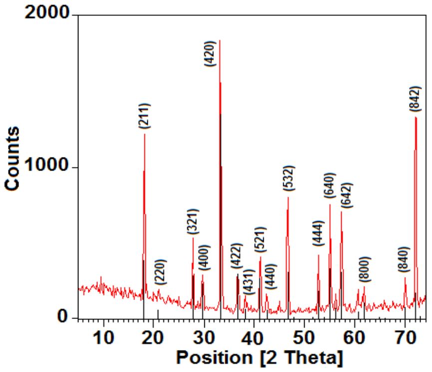

Fig. 3. X-ray diffraction pattern of the grown crystal

It is a little bigger than that of pure YAG (the lattice constant for pure YAG is 12.000 nm [18]), which is due to difference between the atomic radius of Ce^{3+} ions (1.11Å) that occupied the lattice position of the some Y^{3+} ions with 0.93 Å radius in the YAG lattice structure [19]. Fig. 4 shows the absorption spectrum of the prepared sample from the grown crystal under gas limited flowing (present experiment).

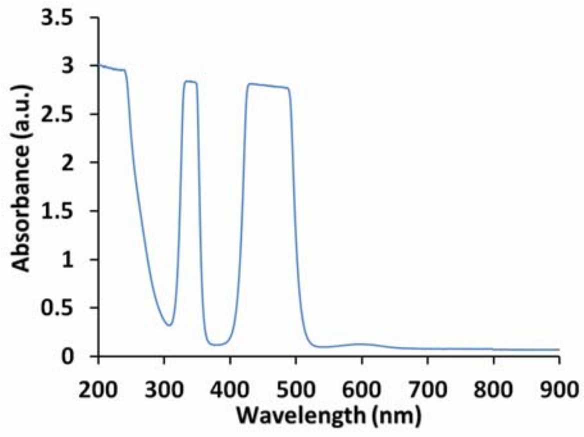

Fig. 4. The absorption spectrum of the Ce:YAG crystal

Three absorption bands located at 222, 340 and 458 nm can be found in the spectrum. These bands belong to the Ce^{3+} ion in the YAG matrix, which has five transitions from the 4f–5d levels [8]. In addition, the absorption band at 255 nm was not observed in absorption spectrum. This band is associated with iron impurity ions [10]. In comparison with other reported results; it can be concluded that the limited gas flowing can be used to reduce Ce^{4+} to Ce^{3+} and exhaust some of the excess oxygen, without using reductive gas such as hydrogen. Rotman and Warde [20] confirmed that two types of lattice defects can be distinguished in Ce:YAG single crystals after annealing in various reducing atmospheres. The presence of these defects leads to a marked increase in the nonluminescent and luminescent defect [20]. The first defect absorbs the light in the wavelength range of 200 to 300 nm without any radiation. The second defect has light emission in a broadband peaking near 320 nm and with broad absorption bands centered near 220 and 250 nm (peak near 235 nm) [20]. To confirm that the mentioned procedure is suitable for the growing of C^{+3}:YAG crystal, the room temperature luminescence spectrum of the sample was recorded in the UV-Vis range. The excitation light wavelength (λ_{ex}) of 255 nm was used and the obtained result is as shown in Fig. 4. There is a broad luminescence band from 470 to 700 nm and no emission peak at 320 nm was observed.

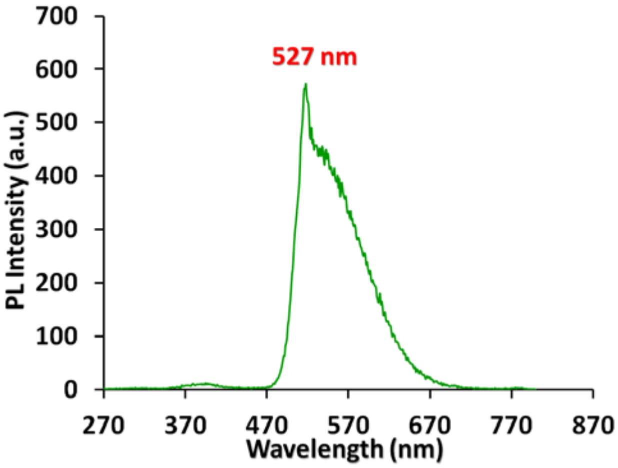

Fig. 5. Photoluminescence spectrum of Ce: YAG sample excited at 255 nm

Previously, it has been reported that the specific feature of Ce-doped $Y_3Al_5O_{12}$ (YAG:Ce) single crystal (SC) is large content of Y_{Al}^{3+} antisite defects (AD). The presence of these defects is an inevitable consequence of high-temperature growth of SC of garnets from melt by the Czochralski or Bridgman methods [21,22]. Zorenko and co-workers [23] studied the nature of the intrinsic emission of $Y_3Al_5O_{12}$, consisting of the excitons and AD luminescence. They believed that the AD existence of Y_{Al}^{3+} type in real crystals of garnets leads to the unusual broadening of spectral lines on RE ions in {c}-positions of garnet lattice. Emission spectrum of YAG SC shows the luminescence of excitons localized around Y_{Al} (AD emission) in the bands peaked at 4.22 eV at 300 K and 4.36 eV at 8 K, respectively. In addition, the luminescence Y_{Al}^{3+} AD in the bands peaked at 3.72 eV at 300 K can be observed. In the luminescence spectrum of the prepared sample, AD emission has not been recorded. The broad luminescence band belongs to transitions from the lowest 5d state to the 4f ground state of the Ce^{3+} ions. Therefore growth conditions were suitable to produce Ce^{3+} ions without any crystalline defects.

The excitation and emission peaks of the color centers are the most typical feature of optical properties of grown Ce:YAG single crystals. Several color-center absorption bands at 235, 296 and 370 nm were reported for Ce:YAG single crystals. Dong et al [10] suggested that the excitation of both the 235 and the 370 nm color center absorption bands results in the same 398 nm emission. Fortunately, the emission band at 398 nm was not recorded in our experimental results. The presence of the color centers was found to cause the reduction of the 550-nm photoluminescence intensity of the Ce^{3+} ion [24]. Experimental results showed that no color-center absorption and emission bands were observed in as-grown Ce:YAG crystal and it is free of usual luminescence crystalline defects. To evaluate the potential application of grown crystal for white LEDs source, the prepared sample was excited by another light wavelength (λ_{ex}=460 nm). The obtained results were shown in figure 5. As shown by Chen et al [25], a free Ce^{3+} ion with $4f^1$ electronic configuration has two ground states, namely $^2F_{5/2}$ and $^2F_{7/2}$. Once with one electron excited from 4f to 5d, the 5d electron of the exited $4f^05d^1$ configuration forms a ^2D term, which is split by spin-orbit coupling and two lower energy levels of $^2D_{3/2}$ and $^2D_{5/2}$ states are formed [24]. Therefore, the excitation band peaked at 460 nm is attributed to $^2F_{5/2}$ (or $^2F_{7/2}$) $\rightarrow {}^2D_{3/2}$ and $^2F_{5/2}$ (or $^2F_{7/2}$) $\rightarrow {}^2D_{5/2}$ transition, respectively [25]. Electrons on the higher energy level of $^2D_{5/2}$ state are unstable, which would relax to $^2D_{3/2}$ state with electron–phonon interaction. Therefore, the emission band in Fig. 5 is attributed to $^2D_{3/2} \rightarrow {}^2F_{7/2}$ or $^2F_{5/2}$ transition. Because the radial wave function of the excited 5d electron extends spatially well beyond the closed $5s^25p^6$, its states are strongly perturbed by the crystal field. Thus, both the strongest excitation band and the strongest emission band are associated with the lowest-lying 5d state, which is affected by crystal field [25].

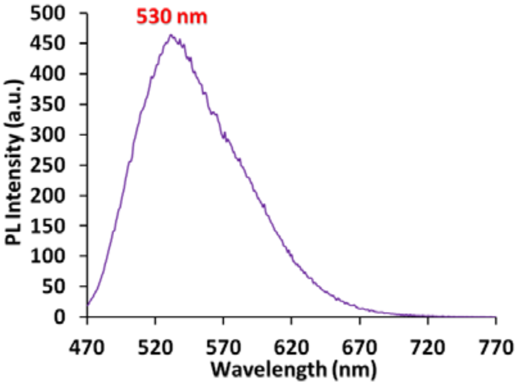

Fig. 6. Photoluminescence spectrum of Ce: YAG sample excited at 460 nm

4. Conclusion

Ce:YAG single crystal was grown under Ar atmosphere with time limited flow. Using XRD analyses, YAG structure was verified and unit cell parameter of the crystal was calculated 12.030 Å. Absorption spectrum of the crystal indicated formation of Ce^{3+} ions in the grown crystal. No color-center absorption and emission bands were observed in as-grown Ce:YAG crystal and it is free of usual luminescence crystalline defects. The as grown crystal is free from lateral core and small central core can be observed in the crystal.

References

[1] E. G. Víllora, S. Arjoca, D. Inomata, K. Shimamura, Proc. SPIE **9768** (2016).

[2] W. Chewpraditkul, L. Swiderski, M. Moszynski, T. Szczesniak, A. Syntfeld-Kazuch, C. Wanarak, P. Limsuwan, IEEE Transactions on Nuclear Science **56** (2009).

[3] S. Arjoca, E.G. Víllora, D. Inomata, K. Aoki, Y. Sugahara, K. Shimamura **2**, 055503 (2015).

[4] Petr Schauer, Nuclear Instruments and Methods in Physics Research B **269,** 2572 (2011).

[5] T. Matsuo, N. Yagi, J. Synchrotron. Radiat. **18,** 601 (2011).

[6] K. Blazek, A. Krasnikov, K. Nejezchleb, M. Nikl, T. Savikhina, S. Zazubovich, Phys. Stat. Sol. B **241,** 1134 (2004).

[7] A. Moszynski, T. Ludziejewski, D. Wolski, W. Klamra, L. Norlin, Nucl. Instr. and Meth. A **345,** 461 (1994).

[8] C. R. Varney, D. T. Mackay, S. M. Reda, F. A. Selim, J. Phys. D: Appl. Phys. **45**, 015103 (2012).

[9] X. Zeng, G. Zhao, J. Xu, H. Li, X. He, H. Pang, M. Y. Jie, J. Cryst. Growth **274**, 495 (2005).

[10] Y. Dong, G. Zhou, J. Xu, G. Zhao, F. Su, L. Su, H. Li, J. Si, X. Qian, X. Li, J. Shen, J. Cryst. Growth **286**, 476 (2006).

[11] G. Zhao, X. Zeng, J. Xu, Y. Xu, Y. Zhou, J. Cryst. Growth **253**, 290 (2003).

[12] C. D. Brandle, J. Cryst. Growth **264**, 593 (2004).

[13] T. H. Kim, Sh. Cho, K. Lee, M. S. Jang, J. H. Ro, Appl. Phys. Lett. **81,** 3756 (2002).

[14] P. Arhipov, S. Tkachenko, S. Vasiukov, K. Hubenko, I. Gerasymov, V. Baumer, A. Puzan, P. Mateychenko, K. Lebbou, O. Sidletskiy, J. Cryst. Growth **449**, 104 (2016).

[15] Jo. Kvapil, Ji. Kvapil, B. Manek, R. Autrata, P. Schauer, J. Cryst. Growth **52**, 542 (1981).

[16] J. Hasani Barbaran, M. R. Ghani Aragi, I. Javaheri, B. Baharvand, M. Tabasi, R. Layegh Ahan, E. Jangjo, Crystallography Reports **60**, 1151 (2015).

[17] L. Schuh, R. Metselaar, J. Eur. Ceram. Soc. **7**, 67 (1991).

[18] Y.-N. Xu, W. Y. Ching, Phys. Rev. B **59**, 10530 (1999).

[19] J. Barzowska, A. Kubicki, M. Grinberg, S. Kaczmarek, Z. Luczynski, A. J. Wojtowicz, Cz. Koepke, Acta Physica Polonica A **95**, 395 (1999).

[20] S. R. Rotman, C. Warde, J. Appl. Phys. **58**, 522 (1985).

[21] M. M. Kuklja, J. Phys. Condens. Matter. **12**, 2953 (2000).

[22] C. R. Stanek, K. J. McClellan, M. R. Levy, R. W. Grimes, Phys. Stat. Sol. (b) **243**, R75 (2006).

[23] Yu. Zorenko, A. Voloshinovskii, V. Savchyn, T. Voznyak, M. Nikl, K. Nejezchleb, V. Mikhailin, V. Kolobanov, D. Spassky, Phys. Stat. Sol. (B) **244**, 2180 (2007).

[24] Jo. Kvapil, Ji. Kvapil, K. Blazek, J. Zikmund, R. Autrata, P. Schauer, Czech J. Phys. B **30**, 185 (1980).

[25] L. Chen, C.-C. Lin, C.-W. Yeh, R.-S. Liu, Materials **3**, 2172 (2010).

---

[*] Corresponding author: jhasani@aeoi.org.ir